Changes of structure and dipole moment of water with temperature and pressure: A first principles study

Dongdong Kang, Jiayu Dai, and Jianmin Yuan[a)]
Department of Physics, College of Science, National University of Defense Technology, Changsha 410073, Hunan, People's Republic of China

(Received 16 February 2011; accepted 17 June 2011; published online 12 July 2011)

The changes of structure and distribution of dipole moment of water with temperatures up to 2800 K and densities up to 2.2 g/cm^3 are investigated using *ab initio* molecular dynamics. Along the isochore of 1.0 g/cm^3, the structure of liquid water above 800 K is dramatically different from that at ambient conditions, where the hydrogen-bonds network collapses. Along the isotherm of 1800 K, the transition from the liquid state to an amorphous superionic phase occurs at 2.0 g/cm^3 (32.9 GPa), which is not observed along the isotherm of 2800 K. With increasing temperature, the average dipole moment of water molecules is decreased arising from the weakened polarization by the collapse of the hydrogen-bonds network, while it is contrarily increased with compression due to the strengthening effect upon the polarization of water molecules. Both higher temperature and pressure broaden the distribution of dipole moment of water molecules due to the enhanced intramolecular charge fluctuations. © *2011 American Institute of Physics*. [doi:10.1063/1.3608412]

I. INTRODUCTION

Water is a special substance which has been paid the most scientific attention among liquids over the past several decades due to its fundamental role in many areas. Despite the apparent simplicity of the water molecule, the condensed phases of water, such as liquid water and ice, are the most mysterious substances in our world.[1] The reason lies in that the highly directional hydrogen bonds (H-bonds) form the complex network, leading to a complex phase diagram with a variety of structural transitions and peculiar physical and chemical properties.[2,3] For example, there are at least 15 crystalline phases for ice confirmed experimentally,[4,5] and new phases are continually predicted in theory.[6] Hitherto great efforts have been made to explore the properties of water,[3] however, the nature of water is far from being fully understood, even the structure of liquid water at ambient conditions is under debate.[7–10]

For recent years, scientists are intensively interested in the behavior of water at extreme conditions because a thick layer of "hot ice" consisting of 56% H_2O in Uranus and Neptune predominantly determines many observable properties of these planets.[11] Therefore the knowledge of water at a wide range of pressures and temperatures is essential for planetary science and fundamental physics. Neutron diffraction and x-ray diffraction, as two main techniques observing the structure of fluid, have provided a lot of detailed information on the structure of liquid water.[12] Furthermore, recent progresses in experimental methods provided more information on the structure of liquid water under high pressures and temperatures.[13] For example, the structure factors of liquid water up to 6.5 GPa and 670 K were measured with neutron diffraction, showing that water approaches a local structure common to simple liquids with increasing density.[14] Weck *et al*. reported evolutions of the structure factor and oxygen coordination number of H_2O and D_2O fluids via x-ray diffraction up to 4.5 GPa and 500 K.[15] Katayama *et al*. extended immediately the x-ray diffraction measurement to 17.1 GPa and 850 K for structure of liquid water along the melting curve.[16] Although experimental advancements have provided more insight into physical properties of water under extreme conditions, it must be stressed that experiments can only access certain areas of the phase diagram due to the limitations of technique. However, theoretical calculations are not restricted in principle, thereby becoming an important way to investigate the properties of water under extreme conditions. *Ab initio* molecular dynamics (MD) simulation has been used to study the properties of matter at high temperatures and densities,[17] and widely applied to simulate the behavior of water cluster and liquid water.[18,19] For example, the study of water up to twofold compression and 2000 K shows the bimolecular mechanism of water dissociation under pressure.[20,21] An exotic superionic phase in the high pressure regime and above 2000 K was predicted, in which the hydrogen atoms diffused rapidly through the solid bcc lattice formed by oxygen atoms.[22] Later, Goncharov[23] and Goldman[24] investigated the superionic phase along the 2000 K isotherm in detail. Schwegler *et al*.[25] found the behavior of the ice-VII phase in the range of 10–50 GPa below melting bore many similarities to a type-II superionic solid because the onset of significant proton diffusion in ice-VII as a function of increasing temperature was gradual. Mattsson and co-workers[26,27] have extended the known phase diagram of water to an extreme density of 15 g/cm^3 and temperatures up to 24 000 K using quantum MD simulations.

The polarization properties of water can be thermodynamically varied as considerably as structural properties at

a)Author to whom correspondence should be addressed. Electronic mail: jmyuan@nudt.edu.cn.

 © 2011 American Institute of Physics

Downloaded 23 Sep 2013 to 202.197.9.8. This article is copyrighted as indicated in the abstract. Reuse of AIP content is subject to the terms at: http://jcp.aip.org/about/rights_and_permissions

high temperatures.[28] The dipole moment of water molecules plays a crucial role in determining the polarization properties. Research on the distributions of molecular dipole moment is therefore essential for exploring the polarization properties of this polar solvent under extreme conditions. As a pioneering work, Silvestrelli and Parrinello[29,30] investigated the change of dipole moment of water molecules passing from the gas to the liquid phase utilizing the maximally localized Wannier functions (MLWFs) and Wannier function centers (WFCs) technique.[31,32] Subsequently, Sharma *et al.*[33,34] investigated both the static and dynamic dielectric properties of liquid and solid water in light of dipolar correlations. The roles of dipole moment of water molecules in salty solutions[35] and narrow pores were also reported.[36] Compared with the abundant knowledge of water at ambient conditions, the information of polarization properties of water under high pressures and temperatures is still scarce, which encourages us to gain more insight into the charge fluctuations and variations of the molecular structure.[37] In addition, although the computer simulations with semiempirical force fields could treat systems containing thousands of atoms, they are limited to a narrow range of the phase diagram due to the validity of the semiempirical force fields. In particular, many force fields for water, taking into account the polarizable effects,[38–40] can only appropriate for the range of moderate temperatures and pressures, approximately up to the supercritical state at most. The requirement of producing a more accurate force field for polarizable and flexible water, which can be applied at a wide range of temperatures and pressures, requires the detailed knowledge of polarization properties of water under extreme conditions as benchmarks. The calculations from first principles thus arise as a main approach to obtain these polarization properties of water.

In this work, we focus on the regime of *P–T* phase diagram in which the proportion of the dissociation of molecules is small. The changes of the structure and dipole moment of water at the temperatures up to 2800 K and the densities up to 2.2 g/cm^3 are therefore reported based on *ab initio* MD simulations. The effects of temperature and pressure on the structure and dipolar distribution of water are investigated along the isochore of 1.0 g/cm^3 and two isotherms of 1800 K and 2800 K, respectively.

II. THEORETICAL METHOD

We performed *ab initio* MD simulations of water using the Car-Parrinello scheme,[41] which was implemented in CPMD package.[42] The electronic structure was determined from the density functional theory by solving the Kohn-Sham equations, and the nuclei propagated around this *ab initio* potential according to Newton's equation of motion because the nuclear quantum effects were expected to be small within the range of *P–T* considered here. For our simulations, the Becke-Lee-Yang-Parr (BLYP)[43,44] functional was used to treat the exchange-correlation interaction between electrons, which has been shown to give a good description of structural and electronic properties of water.[45] The interaction between the core and valence electrons was described by Troullier-Martins norm-conserving pseudopotential[46] with a plane-wave cutoff of 120 Ry, giving a good convergence of pressure.[24] The Brillouin zone was sampled at the Γ point only.

The simulated system consisted of 32 H_2O molecules in a cubic supercell with periodic boundary conditions. The size effects were found to be rather small at ambient conditions.[45] Here bigger box containing 64 H_2O molecules was tested at highest density in our simulations and no significant difference was found. The size of box was 9.86 Å for 1.0 g/cm^3, which was rescaled according to different densities. The constant *NVT* simulations were performed and the temperature was controlled via a Nosé-Hoover-chain thermostats.[47] A conservative value of 200 a.u. for the fictitious electronic mass with 2.5 a.u. (0.06 fs) for the time step were chosen to ensure the validity of adiabatic conditions for electrons in the whole MD process. For the isochore of 1.0 g/cm^3, the temperature was increased from 300 K to 2800 K with an increment of several hundred Kelvin, while for the isotherms of 1800 K and 2800 K, the configuration was compressed from 1.0 g/cm^3 to 2.2 g/cm^3 with a sequential step of 0.2 g/cm^3. For each ρ-T point the configuration was equilibrated for 2 ps at least and a production simulation was run for 7 ps.

The structural properties of water were characterized by the radial distribution function (RDF), which quantified the probability of one atom being located at a certain distance from another atom in coordination space. The dipole moment of water molecules was calculated using the method of MLWFs, which were obtained from the Bloch orbitals available via a unitary transformation. According to this method, we could partition the total charge into individual molecular contributions.[29,31] At each time step the instantaneous static molecular dipole for the ith molecule in the cell is defined as:[37]

$$\boldsymbol{\mu}_i = \mathbf{R}_{\mathrm{H}_1} + \mathbf{R}_{\mathrm{H}_2} + 6\mathbf{R}_{\mathrm{O}} - 2\sum_{s=1}^{4} \mathbf{R}_{\mathrm{W}_s}, \tag{1}$$

where $\mathbf{R}_{\mathrm{O}}$, $\mathbf{R}_{\mathrm{H}_1}$, $\mathbf{R}_{\mathrm{H}_2}$ are the nulcear coordinates of the ith molecule, respectively, and $\mathbf{R}_{\mathrm{W}_s}$, $s = 1, \ldots, 4$ are the corresponding WFCs. Two MLWFs are centered on the OH covalent bonds and the other two are lone pairs centered on the remaining approximately tetrahedral directions. It must be noted that at high temperatures and pressures, although the total amount of dissociated molecules is small at the *P–T* range considered here,[21] water molecules are in dynamical equilibration between dissociating and recombining. At each time step, we used a dissociation criterion of coordination number of oxygen atoms. The hydrogen atoms are assigned to a certain molecule if the distance of OH is less than the cutoff at which the coordination number $n_{\mathrm{OH}}(r)$ of oxygen atom is equal to 2. The other dissociated molecules are excluded in our calculations for dipole moment.

To identify the structural changes of water with increasing temperature and pressure, we calculated the RDFs and the orientation order parameter Q, which is defined as:[48]

$$Q = 1 - \frac{3}{8}\sum_{i=1}^{3}\sum_{j=i+1}^{4}\left(\cos\theta_{ij} + \frac{1}{3}\right)^2, \tag{2}$$

where θ_{ij} is the angle subtended at the central oxygen atom between the ith and jth bonds. The value of Q varies

Downloaded 23 Sep 2013 to 202.197.9.8. This article is copyrighted as indicated in the abstract. Reuse of AIP content is subject to the terms at: http://jcp.aip.org/about/rights_and_permissions

between 0 (in an ideal gas) and 1 (in a perfect tetrahedral network), which can be used as a measure of tetrahedrality for local coordination structure.[52] In addition, deeper insights on the local arrangement of molecular geometry were achieved through analyzing the distribution of the length and angle of OH covalent bonds and H-bonds in simulation systems.

III. RESULTS AND DISCUSSION

A. Properties along the isochore of 1.0 g/cm^3

To shed light on the effects of temperature on the water structure, we have performed the *ab initio* MD simulations along an isochore of 1.0 g/cm^3, and presented the RDFs of water at different temperatures in Fig. 1. For the oxygen-oxygen RDF at 300 K, the first peak, second peak, and first minimum are at the position of 2.77, 4.45, and 3.3 Å, respectively, which are in good agreement with x-ray scattering[49] and neutron diffraction[50] measurements. The coordination number $n_{OO}(r)$ under the first peak of $g_{OO}(r)$ is 4.1, indicating that the liquid water keeps the ordered arrangement with four nearest neighbor molecules surrounding a center one. The OH covalent bonds and H-bonds at 300 K, characterized by the first two peaks of $g_{OH}(r)$, are 0.98 and 1.77 Å, also consistent with the previous experiment.[51]

With increasing temperature, the first peak of $g_{OO}(r)$ is broadened considerably, but its position remains essentially fixed, with a small outward shift (i.e., shifting to larger value) of 0.1 Å. The second and third peaks almost disappear at 500 K, indicating that these two coordination shells collapse with raising temperature. Although the intensity of the first peak reduces gradually, the feature of oxygen-oxygen RDFs becomes very similar above 800 K. They are characterized by a largely broadened peak and an extensively covering peak at about 5.6 Å. The coordination number of the first coordination shell reaches 12 at 2800 K compared with 4.1 at ambient condition, and it seems that the first two coordination shells merge into single one. The reason lies in that it is becoming easier to overcome the bound of H-bonds for thermal excited water molecules, thereby the tetrahedral H-bonds network collapses dramatically and the liquid water approaches homogeneity at high temperatures, as revealed from the second peak of $g_{OH}(r)$. One can see that the second and third peaks in $g_{OH}(r)$ become merging above 800 K, in good agreement with the calculations by Ikeda *et al.*[52] In addition, the first minimal value of $g_{OH}(r)$ is slightly larger than zero to indicate the occurrence of dissociations of water molecules.

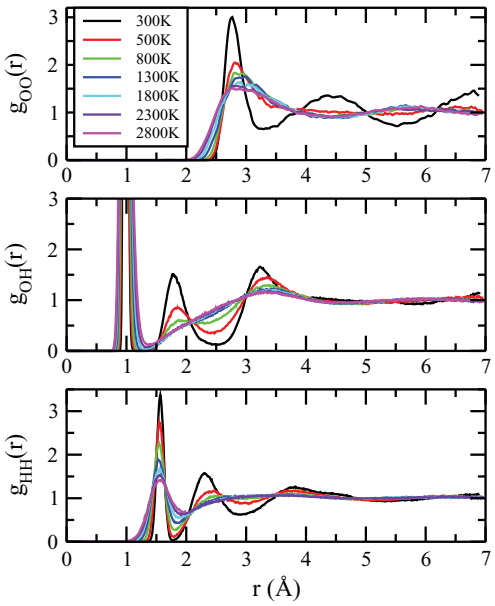

FIG. 1. Radial distribution functions of water at $\rho = 1.0$ g/cm^3 from 300 K to 2800 K calculated from our *ab initio* simulations.

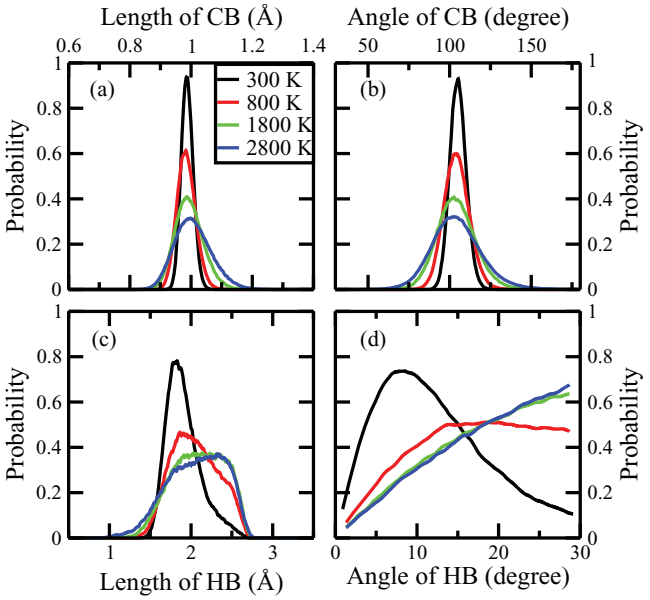

FIG. 2. Distributions of the bond length and angle of OH covalent bonds (CB) and H-bonds (HB) at $\rho = 1.0$ g/cm^3 from 300 K to 2800 K.

In order to gain a further insight into the structural changes of water as is heated, we present the orientation order parameter Q and average number of H-bonds per water molecule in Table I. The average number of H-bonds per water molecule is obtained through total number of H-bonds divided by total number of water molecules in the simulation box. In the present work, a geometrical criterion of H-bonds[53] is used, i.e., the distance between related oxygen atoms is less than 3.5 Å and the hydrogen-donor-acceptor angle (i.e., H-bonds angle) is less than 30°. One can see that with increasing temperature, the average number of H-bonds per water molecule is reduced from 1.85 at 300 K to 1.19 at 800 K, and finally 0.8 at 2800 K. It indicates that the number of H-bonds formed between the first-shell molecules and the central molecule are decreased. Meanwhile, the number of interstitial molecules which are not hydrogen-bonded (H-bonded) to any of the first-shell molecules are increased correspondingly. The orientation order parameter varies from 0.72 at 300 K to 0.46 at 800 K, and maintains about 0.4 above 800 K, showing that the ideal tetrahedral coordination of water molecules collapses at 800 K. It is consistent with Ref. 52 and the above analysis of RDFs. The distributions of the bond length and angle of OH covalent bonds and H-bonds with increasing temperature are shown in Fig. 2. One can see clearly

Downloaded 23 Sep 2013 to 202.197.9.8. This article is copyrighted as indicated in the abstract. Reuse of AIP content is subject to the terms at: http://jcp.aip.org/about/rights_and_permissions

TABLE I. The orientation order parameter Q, average number of H-bonds per water molecule (No. of HB) and average dipole moment of water molecules corresponding to different densities along the isochore of 1.0 g/cm^3.

T (K)	300	800	1800	2800
Q	0.72	0.46	0.40	0.39
No. of HB	1.85	1.19	0.87	0.80
Dipole (Debye)	3.00	2.64	2.42	2.37

that both the intramolecular geometry and intermolecular H-bonds arrangement are influenced significantly when the system is heated. With increasing temperature, the length of OH covalent bonds reaches over wider range as well as the angle between two OH covalent bonds. Their distribution broadens dramatically, indicating that water molecules can be distorted significantly at high temperature. As for H-bonds, due to their weak nature, the H-bonds geometry is distorted more easily than intramolecular geometry, as shown in Figs. 2(c) and 2(d). The peak of distribution of H-bonds length shifts to larger value, and more importantly, it becomes more and more flat as temperature is raised. The distribution of H-bonds angle exhibits a significant change. Above 800 K, the peak of distribution of H-bonds angle shifts out of the range of H-bonds angle definition ($0 \sim 30^\circ$), and it distributes almost linearly at higher temperatures. This arises apparently from the strengthened librational motion of water molecules. It can be concluded from above analyses that the tetrahedral H-bonds network exhibits collapse above 800 K, where almost half the H-bonded molecules are transformed to be interstitial molecules.

The effect of temperature on polarization properties of liquid water is presented by the distribution of dipole moment of water molecules in Fig. 3. In order to test the validity of our calculations, we first compare the average dipole moment at 300 K obtained here with theoretical value[29] of 2.95 Debye (D) and experimental value[54] 2.9 $\pm$ 0.6 D, showing an excellent agreement. With raising temperature, the peak of dipole moment shifts towards small value, approaching the experimental value 1.86 D in the gas phase,[55] and the intensity reduces concurrently. The average dipole moment (shown in Table I) and half maximal width (HMW) of distribution

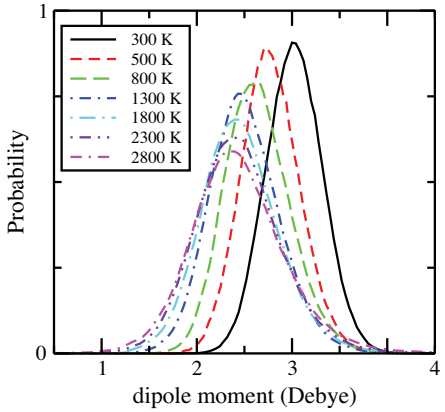

FIG. 3. Distributions of the modulus of the water molecular dipole moment at $\rho = 1.0$g/cm^3 from 300 K to 2800 K.

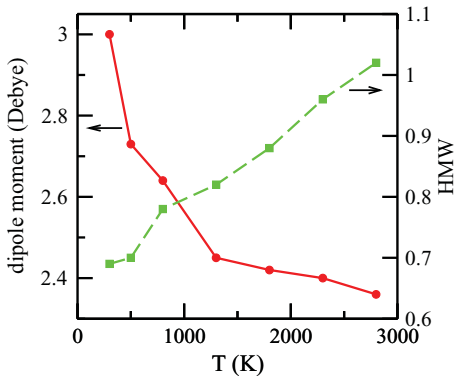

FIG. 4. Temperature dependence of the average dipole moment (solid line) and half maximal width (HMW) (dashed line) of distribution functions corresponding to Fig. 2.

functions at different temperatures are displayed in Fig. 4. It is clearly shown that the average dipole moment drops dramatically up to 1300 K, and continues to decrease with a small slope. Meanwhile, the HMW increases approximately linearly. In condensed phases of water, the internal electric field arising from the interaction of water molecules with the surrounding ones polarizes the water molecules, which leads to a large dipole moment relative to that in the gas phase. As temperature is raised, the average number of H-bonds per molecule is significantly decreased and the local tetrahedral H-bonds network dramatically collapses, leading to water molecules more free than at ambient conditions. Thus the polarization interaction between water molecules is weakened and the peak of dipole moment shifts approaching the value in gas phase. Meanwhile, the vibrational amplitudes of OH bonds increase with rising temperature (shown in Fig. 2), leading to more intense charge fluctuations in water molecules at higher temperatures. Thus the distribution of dipole moment broadens dramatically and covers a wide range at high temperatures.

B. Properties along the isotherms of 1800 K and 2800 K

Two isotherms of 1800 K and 2800 K were chosen to investigate the effects of pressure on the structural and polarization properties of water. The calculated pressures

TABLE II. The orientation order parameter Q, average number of H-bonds per water molecule (No. of HB), average dipole moment of water molecules and pressure P corresponding to different densities along the isotherms of 1800 K and 2800 K.

	ρ (g/cm^3)	1.0	1.2	1.4	1.6	1.8	2.0	2.2
1800 K	P (GPa)	4.4	7.1	11.7	17.5	25.4	32.9	42.9
	Q	0.40	0.42	0.42	0.43	0.42	0.37	0.38
	No. of HB	0.87	0.90	0.96	1.01	1.04	1.02	1.02
	Dipole (Debye)	2.42	2.49	2.66	2.81	2.91	3.06	3.21
2800 K	P (GPa)	6.5	9.4	14.4	20.9	29.1	39.4	51.7
	Q	0.39	0.40	0.41	0.42	0.42	0.42	0.40
	No. of HB	0.80	0.83	0.87	0.92	0.96	0.95	0.97
	Dipole (Debye)	2.36	2.48	2.62	2.82	3.00	3.10	3.20

Downloaded 23 Sep 2013 to 202.197.9.8. This article is copyrighted as indicated in the abstract. Reuse of AIP content is subject to the terms at: http://jcp.aip.org/about/rights_and_permissions

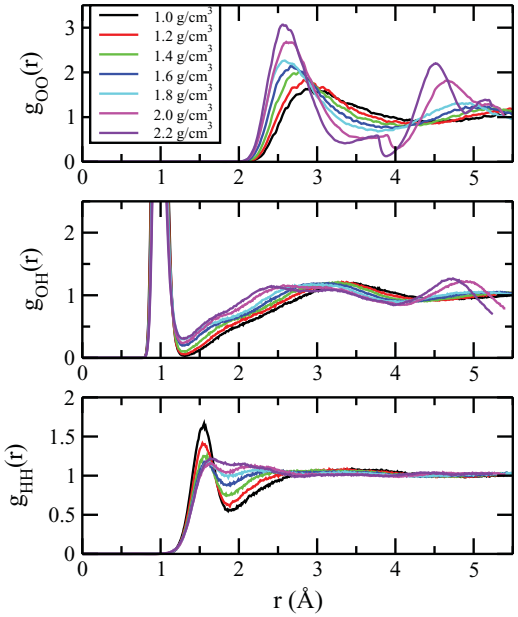

FIG. 5. Radial distribution functions of water at 1800 K from 1.0 g/cm^3 to 2.2 g/cm^3 determined from our *ab initio* simulations.

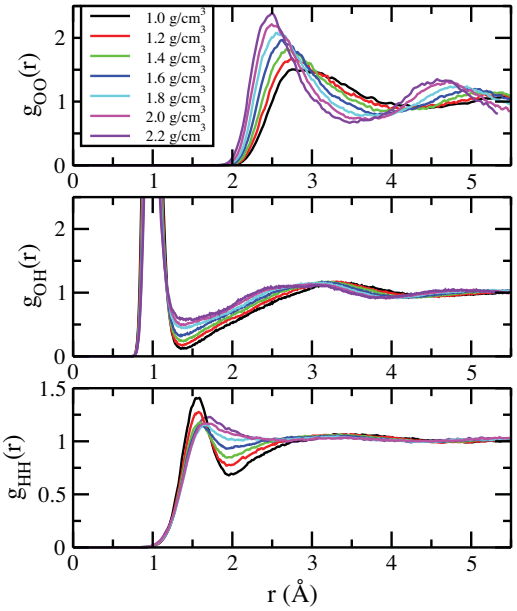

FIG. 7. Radial distribution functions of water at 2800 K from 1.0 g/cm^3 to 2.2 g/cm^3.

corresponding to different densities are listed in Table II. In Fig. 5, the RDFs of water at 1800 K under high pressures up to 42.9 GPa are displayed. Below 1.8 g/cm^3 (25.4 GPa), the main change in $g_{OO}(r)$ is the inward shifts in the position of the first two peaks with sharpening. A most dramatic change occurs above 2.0 g/cm^3 (32.9 GPa), where a small peak appears between the two main peaks. Also a similar small peak is observed after the second peak. It indicates that water has a more ordered structure under larger compression, further evidenced by the analysis of configurations during the simulations. We calculated the mean square displacement of oxygen and hydrogen atoms of water at 1.0 g/cm^3 and 2.0 g/cm^3, respectively, and showed the results in Fig. 6. One can clearly see that at the density of 1.0 g/cm^3, hydrogen and oxygen atoms have the same diffusive properties, whereas at 2.0 g/cm^3 hydrogen atoms become much more highly diffusive than oxygen atoms. According to the relation

$$6D = \lim_{t\to\infty} \frac{d}{dt}\langle|\mathbf{r}_i(t) - \mathbf{r}_i(0)|^2\rangle, \tag{3}$$

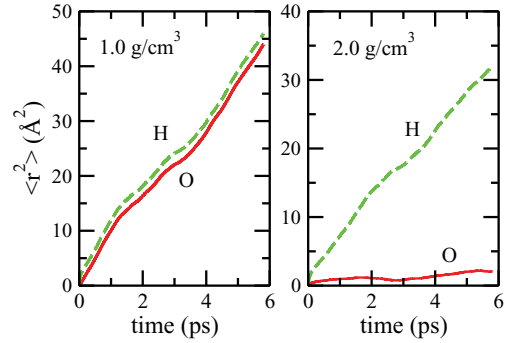

FIG. 6. The mean square displacement of oxygen (solid line) and hydrogen (dashed line) atoms of water at 1800 K for 1.0 g/cm^3 (left panel) and 2.0 g/cm^3 (right panel).

the diffusion coefficient D at 2.0 g/cm^3 is 0.4×10^{-5} cm^2/s for oxygen atoms and 8.5×10^{-5} cm^2/s for hydrogen atoms compared to 11.5×10^{-5} cm^2/s and 11.6×10^{-5} cm^2/s at 1.0 g/cm^3, respectively. The feature of highly diffusive hydrogen atoms is also shown in $g_{HH}(r)$ of Fig. 5, where at 2.2 g/cm^3, hydrogen atoms exhibit more disorder instead of short-range order at lower densities. At first sight, above 2.0 g/cm^3 at 1800 K, water is likely to be in the superionic phase, where the oxygen atoms vibrate around their solid lattice positions and hydrogen atoms are hopping among oxygen atoms. It must be pointed out that the lattice formed by oxygen atoms presented here is not the perfect bcc solid lattice and distorts slowly during simulations. Moreover, the diffusion coefficient of hydrogen atoms even at 2.2 g/cm^3 is lower than 10^{-4} cm^2/s, which is an important feature of superionic state.[24,56] These indicate that the state considered here is the amorphous superionic phase, which is a transition state from the liquid phase to the solid bcc superionic phase.[22] The condition (32.9 GPa, 1800 K), at which the amorphous superionic phase occurs, accords with the theoretical prediction.[22] However, the pressure is lower than that in calculations by Goldman.[24] This may be due to their use of a bigger supercell in simulations. Under compression, the position of the first peak in $g_{OH}(r)$ remains nearly fixed, indicating that the length of OH covalent bonds in nondissociative water molecules is nearly not affected up to 42.9 GPa (2.2 g/cm^3). The first minimal value becomes substantially larger than zero, revealing that the amount of the dissociated molecules becomes increasing. The RDFs at 2800 K (shown in Fig. 7) are very similar to that at 1800 K. The major difference is that the amorphous superionic phase does not occur at 2800 K, compared with 1800 K. This is due to the fact that an increase of temperature leads to the melting of the oxygen amorphous structure. At 2800 K the superionic phase may appear at higher pressure, at least above 52 GPa.

For the sake of understanding the structural change at high temperatures and pressures at molecular level, we

Downloaded 23 Sep 2013 to 202.197.9.8. This article is copyrighted as indicated in the abstract. Reuse of AIP content is subject to the terms at: http://jcp.aip.org/about/rights_and_permissions

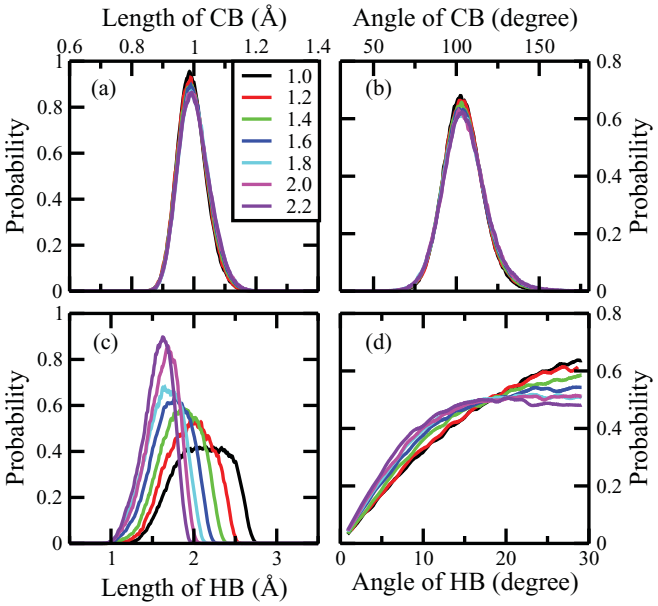

FIG. 8. Distributions of the bond length and angle of OH covalent bonds (CB) and H-bonds (HB) at 1800 K from 1.0 g/cm^3 to 2.2 g/cm^3.

calculated the orientation order parameter Q and average number of H-bonds per molecule, which are listed in Table II. Here, a geometrical criteria of H-bonds, similar to that of 1.0 g/cm^3 water, is used. The H-bonds angle criterion is still 30°, while the H-bonds length is rescaled according to the compression ratio. From Table II, one can see that Q keeps almost fixed around 0.4 at both 1800 K and 2800 K, thereby it can be inferred that the local arrangement of four nearest neighbor molecules around a central molecule seems to have a minor dependence on pressure. However, the motion of water molecules is somewhat influenced by compression. The slowly increasing average number of H-bonds per molecule indicates that compression enhances the interaction between the nearest neighbor molecules, as is illustrated in Fig. 8. The peak of distribution of H-bonds length is dramatically enhanced and the main part of the distribution of H-bonds angle shifts to small value with increasing pressure. It reveals that the reorientation of water molecules becomes slowed down due to the enhanced interaction between molecules as pressure is raised. On the contrary, compression has almost no influence on the intramolecular geometry, as shown in Figs. 8(a) and 8(b). At 2800 K, both the intramolecular and intermolecular geometries are very similar to that at 1800 K.

In order to explore the effect of pressure on polarization properties of liquid water, we calculated the distribution of dipole moment of water molecules and showed the results in Figs. 9 and 10 for two isotherms of 1800 K and 2800 K, respectively. The average dipole moments are also presented in Table II. With increasing pressure, the peaks of dipole moments shift from 2.42 D at 4.4 GPa to 3.21 D at 42.9 GPa for the isotherm of 1800 K, while at 2800 K, they shift from 2.36 D at 6.5 GPa to 3.2 D at 51.7 GPa. Meanwhile, the distribution function of dipole moment broadens considerably. From Figs. 9 and 10, one can see that the maximal dipole moment of water molecules reaches to 6.0 D, even beyond 6.0 D at 2800 K and 2.2 g/cm^3, although the minima

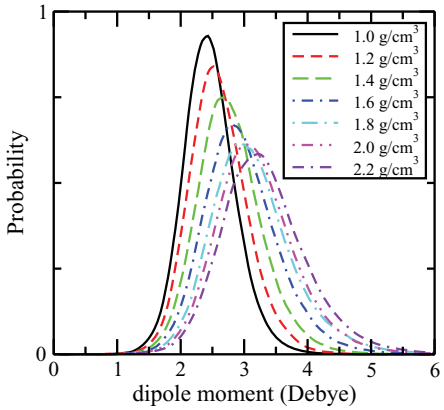

FIG. 9. Distributions of the modulus of the water molecular dipole moment at 1800 K from 1.0 g/cm^3 to 2.2 g/cm^3.

maintain about 1.0 D substantially. In contrast to the weakening effects of temperature on polarization, compression decreases the average distances between water molecules, and therefore strengthens the polarization between the nearest neighbor water molecules. Although the intramolecular geometry is not sensitive to compression below 2.2 g/cm^3 (shown in Fig. 8), the significantly enhanced intermolecular interaction weakens librational motion of water molecules with increasing pressure, thereby causing the polarization between neighbor molecules dramatically enhanced. Therefore, the average dipole moment is increased with rising pressure. From above analysis, we can see that both the temperature and pressure enhance charge fluctuations in water molecules. In this sense, they have the same effects on the polarization of water molecules.

In addition, at high temperatures and pressures the highly diffusive hydrogen atoms make water molecules dissociate and recombine quickly. The dissociation can be characterized by the RDFs between oxygen and its nearest MLWF centers. The results for the isotherm of 2800 K are shown in Fig. 11. The two peaks, corresponding to lone pairs and OH covalent bond orbitals, respectively, become broader with increasing pressure. The position of the first peak keeps fixed substantially, while the second peak shifts inwards, indicating that

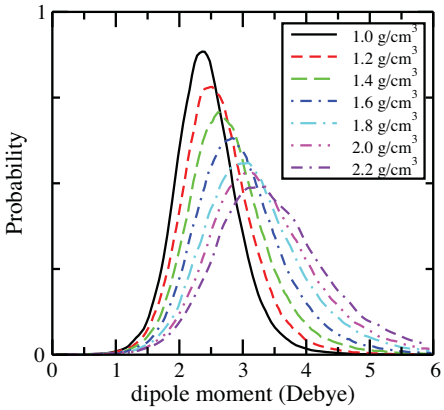

FIG. 10. Distributions of the modulus of the water molecular dipole moment at 2800 K from 1.0 g/cm^3 to 2.2 g/cm^3.

Downloaded 23 Sep 2013 to 202.197.9.8. This article is copyrighted as indicated in the abstract. Reuse of AIP content is subject to the terms at: http://jcp.aip.org/about/rights_and_permissions

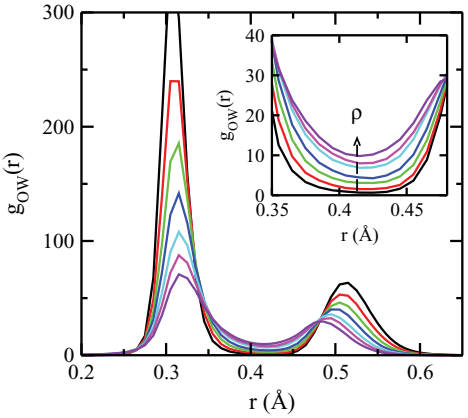

FIG. 11. The radial distribution function between oxygen and its nearest maximally localized Wannier function centers at 2800 K from 1.0 g/cm^3 to 2.2 g/cm^3. The inset shows the results between 0.35 Å and 0.48 Å, in which the dashed arrow indicates the increasing density. The representations of the types of lines are the same as those in Fig. 6

the length of OH covalent bonds reduces slightly up to 2.2 g/cm^3. An important change is that the minimum between the two peaks rises with increasing density. It indicates the existence of the dissociation and an increasing concentration of ions H_3O^+ and OH^- due to the bimolecular process.[21]

IV. CONCLUSIONS

In this paper, we have investigated the structure and distribution of dipole moment of water at temperatures up to 2800 K and pressures up to 52 GPa using *ab initio* MD simulations. Results show that the structure of liquid water above 800 K is dramatically different from that at ambient conditions. The first two coordination shells of oxygen merge to one shell because the tetrahedral H-bonds network collapses with increasing temperature. At 32.9 GPa along the isotherm of 1800 K, a transition from the liquid state to an amorphous superionic phase occurs, which does not appear along the isotherm of 2800 K. The distribution of the molecular dipole moment broadens with increasing temperature and pressure due to the enhanced intramolecular charge fluctuations. In this sense, both the temperature and pressure have the similar effects on the polarization properties of water. However, the average dipole moment of water molecules increases with larger pressure, but decreases with higher temperature. In addition, the water molecular dissociation can be characterized by the first minimum value in oxygen-oxygen RDF, which is larger than zero, and also by the RDF between oxygen atoms and their nearest MLWF centers.

ACKNOWLEDGMENTS

This work is supported by the National Natural Science Foundation of China under Grant Nos. 10734140 and 60921062, the National Basic Research Program of China (973 Program) under Grant No. 2007CB815105. Calculations are carried out at the Research Center of Supercomputing Application, NUDT.

[1] A. K. Soper, Science **297**, 1288 (2002).
[2] P. Ball, Nature (London) **452**, 291 (2008).
[3] C. A. Angell, Science **319** 582 (2008).
[4] G. Malenkov, J. Phys.: Condens. Matter **21**, 283101 (2009).
[5] C. G. Salzmann, P. G. Radaelli, E. Mayer, and J. L. Finney, Phys. Rev. Lett. **103**, 105701 (2009).
[6] B. Militzer and H. F. Wilson, Phys. Rev. Lett. **105**, 195701 (2010).
[7] Ph. Wernet, D. Nordlund, U. Bergmann, M. Cavalleri, M. Odelius, H. Ogasawara, L. Å. Näslund, T. K. Hirsch, L. Ojamäe, P. Glatzel, L. G. M. Pettersson, and A. Nilsson, Science **304**, 995 (2004).
[8] J. D. Smith, C. D. Cappa, K. R. Wilson, B. M. Messer, R. C. Cohen, and R. J. Saykally, Science **306**, 851 (2004).
[9] C. Huang, K. T. Wikfeldt, T. Tokushima, D. Nordlund, Y. Harada, U. Bergmann, M. Niebuhr, T. M. Weiss, Y. Horikawa, M. Leetmaa, M. P. Ljungberg, O. Takahashi, A. Lenz, L. Ojamae, A. P. Lyubartsev, S. Shin, L. G. M. Pettersson, and A. Nilsson, Proc. Natl. Acad. Sci. U.S.A. **106**, 15214 (2009).
[10] A. K. Soper, J. Teixeira, and T. Head-Gordon, Proc. Natl. Acad. Sci. U.S.A. **107**, E44 (2010).
[11] W. B. Hubbard, Science **214**, 145 (1981).
[12] A. K. Soper, J. Phys.: Condens. Matter **19**, 335206 (2007).
[13] A. F. Goncharov and R. J. Hemley, Chem. Soc. Rev. **35**, 899 (2006).
[14] Th. Strassle, A. M. Saitta, Y. Le Godec, G. Hamel, S. Klotz, J. S. Loveday, and R. J. Nelmes, Phys. Rev. Lett. **96**, 067801 (2006).
[15] G. Weck, J. Eggert, P. Loubeyre, N. Desbiens, E. Bourasseau, J.-B. Maillet, M. Mezouar, and M. Hanfland, Phys. Rev. B **80**, 180202(R) (2009).
[16] Y. Katayama, T. Hattori, H. Saitoh, T. Ikeda, and K. Aoki, Phys. Rev. B **81**, 014109 (2010).
[17] J. Y. Dai, Y. Hou, and J. M. Yuan, Phys. Rev. Lett. **104**, 245001 (2010); Astrophys. J. **721**, 1158 (2010).
[18] D. D. Kang, J. Y. Dai, Y. Hou, and Y. M. Yuan, J. Chem. Phys. **133**, 014302 (2010).
[19] J. Y. Dai, and J. M. Yuan, Europhys. Lett. **88**, 20001 (2009).
[20] E. Schwegler, G. Galli, and F. Gygi, Phys. Rev. Lett. **84**, 2429 (2000).
[21] E. Schwegler, G. Galli, F. Gygi, and R. Q. Hood, Phys. Rev. Lett. **87**, 265501 (2001).
[22] C. Cavazzoni, G. L. Chiarotti, S. Scandolo, E. Tosatti, M. Bernasconi, and M. Parrinello, Science **283**, 44 (1999).
[23] A. F. Goncharov, N. Goldman, L. E. Fried, J. C. Crowhurst, I-Feng W. Kuo, C. J. Mundy, and J. M. Zaug, Phys. Rev. Lett. **94**, 125508 (2005).
[24] N. Goldman, L. E. Fried, I-Feng W. Kuo, and C. J. Mundy, Phys. Rev. Lett. **94**, 217801 (2005).
[25] E. Schwegler, M. Sharma, F. Gygi, and G. Galli, Proc. Natl. Acad. Sci. U.S.A. **105**, 14779 (2008).
[26] T. R. Mattsson and M. P. Desjarlais, Phys. Rev. Lett. **97**, 017801 (2006).
[27] M. French, T. R. Mattsson, N. Nettelmann, and R. Redmer, Phys. Rev. B **79**, 054107 (2009).
[28] M. Boero, K. Terakura, T. Ikeshoji, C. C. Liew, and M. Parrinello, Phys. Rev. Lett. **85**, 3245 (2000).
[29] P. L. Silvestrelli and M. Parrinello, Phys. Rev. Lett. **82**, 3308 (1999).
[30] P. L. Silvestrelli and M. Parrinello, J. Chem. Phys. **111**, 3572 (1999).
[31] N. Marzari and D. Vanderbilt, Phys. Rev. B **56**, 12847 (1997).
[32] P. L. Silvestrelli, N. Marzari, D. Vanderbilt, and M. Parrinello, Solid State Commun. **107**, 7 (1998).
[33] M. Sharma, R. Resta, and R. Car, Phys. Rev. Lett. **98**, 247401 (2007).
[34] W. Chen, M. Sharma, R. Resta, G. Galli, and R. Car, Phys. Rev. B **77**, 245114 (2008).
[35] R. Scipioni, D. A. Schmidt, and M. Boero, J. Chem. Phys. **130**, 024502 (2009).
[36] C. Dellago and M. M. Naor, Comput. Phys. Commun. **169**, 36 (2005).
[37] M. Sharma, R. Resta, and R. Car, Phys. Rev. Lett. **95**, 187401 (2005).
[38] W. L. Jorgensen, J. Chandrasekhar, J. D. Madura, R. W. Impey, and M. L. Klein, J. Chem. Phys. **79**, 926 (1983).
[39] M. W. Mahoney and W. L. Jorgensen, J. Chem. Phys. **112** 8910 (2000).
[40] G. S. Fanourgakis and S. S. Xantheas, J. Chem. Phys. **128**, 074506 (2008).
[41] R. Car and M. Parrinello, Phys. Rev. Lett. **55**, 2471 (1985).
[42] CPMD version 3.13.2, http://www.cpmd.org/, Copyright IBM Corp 1990–2008, Copyright MPI für Festkörperforschung Stuttgart 1997–2001.
[43] A. D. Becke, Phys. Rev. A **38**, 3098 (1988).
[44] C. Lee, W. Yang, and R. G. Parr, Phys. Rev. B **37**, 785 (1988).
[45] J. Grossman, E. Schwegler, E. W. Draeger, F. Gygi, and G. Galli, J. Chem. Phys. **120**, 300 (2004).
[46] N. Troullier and J. Martins, Phys. Rev. B **43**, 1993 (1991).

Downloaded 23 Sep 2013 to 202.197.9.8. This article is copyrighted as indicated in the abstract. Reuse of AIP content is subject to the terms at: http://jcp.aip.org/about/rights_and_permissions

[47]G. J. Martyna, M. L. Klein, and M. Tuckerman, J. Chem. Phys. **97**, 2635 (1992).
[48]J. R. Errington and P. G. Debenedetti, Nature (London) **409**, 318 (2001).
[49]J. M. Sorenson, G. Hura, R. M. Glaeser, and T. Head-Gordon, J. Chem. Phys. **113**, 9149 (2000).
[50]A. K. Soper, Chem. Phys. **258**, 121 (2000).
[51]K. Ichikawa, Y. Kameda, T. Yamaguchi, H. Wakita, and M. Misawa, Mol. Phys. **73**, 79 (1991).
[52]T. Ikeda, Y. Katayama, H. Saitoh, and K. Aoki, J. Chem. Phys. **132**, 121102 (2010).
[53]C. Caleman and D. van der Spoel, J. Chem. Phys. **125**, 154508 (2006).
[54]Y. S. Badyal, M.-L. Saboungi, D. L. Price, S. D. Shastri, D. R. Haeffner, and A. K. Soper, J. Chem. Phys. **112**, 9206 (2000).
[55]S. A. Clough, Y. Beers, G. P. Klein, and L. S. Rothman, J. Chem. Phys. **59**, 2254 (1973).
[56]E. Katoh, H. Yamawaki, H. Fujihisa, M. Sakasita, and K. Aoki, Science **295**, 1264 (2002).

Downloaded 23 Sep 2013 to 202.197.9.8. This article is copyrighted as indicated in the abstract. Reuse of AIP content is subject to the terms at: http://jcp.aip.org/about/rights_and_permissions